ARTICLES

Positive feedback of G1 cyclins ensures coherent cell cycle entry

Jan M. Skotheim[1], Stefano Di Talia[1], Eric D. Siggia[1] & Frederick R. Cross[2]

In budding yeast, *Saccharomyces cerevisiae*, the Start checkpoint integrates multiple internal and external signals into an all-or-none decision to enter the cell cycle. Here we show that Start behaves like a switch due to systems-level feedback in the regulatory network. In contrast to current models proposing a linear cascade of Start activation, transcriptional positive feedback of the G1 cyclins Cln1 and Cln2 induces the near-simultaneous expression of the ~200-gene G1/S regulon. Nuclear Cln2 drives coherent regulon expression, whereas cytoplasmic Cln2 drives efficient budding. Cells with the *CLN1* and *CLN2* genes deleted frequently arrest as unbudded cells, incurring a large fluctuation-induced fitness penalty due to both the lack of cytoplasmic Cln2 and insufficient G1/S regulon expression. Thus, positive-feedback-amplified expression of Cln1 and Cln2 simultaneously drives robust budding and rapid, coherent regulon expression. A similar G1/S regulatory network in mammalian cells, comprised of non-orthologous genes, suggests either conservation of regulatory architecture or convergent evolution.

Positive feedback in genetic control networks can ensure that cells do not slip back and forth between either cell cycle phases or developmental fates. For example, commitment to sporulation in budding yeast is driven by transcriptional positive feedback of the meiotic inducer *IME1* (refs 1–3). In *Xenopus laevis*, positive feedback underlies the all-or-none characteristics of oocyte maturation[4,5] and mitotic entry[6,7], suggesting the frequent use of positive feedback to regulate cellular transitions.

Absent from this list of examples is the well-studied Start checkpoint controlling cell cycle commitment in budding yeast. Nutrient limitation and pheromone exposure arrest cells before DNA replication, whereas size control extends G1 in small daughter cells[8–11]. Beyond Start, cells proceed through division almost independently of size and environment[9]. Previous experiments suggested that Start represents a feedback-free cascade of events[12] (see schematic in Fig. 1a; omitting red arrows). The transition is initiated by the G1 cyclin Cln3 (refs 13–15), which in complex with Cdc28 activates the transcription of about 200 genes[16] by phosphorylating promoter-bound protein complexes that include the transcription factors SBF and MBF[17] and the transcriptional inhibitor Whi5 (refs 18 and 19). Phosphorylation and inactivation of Whi5 is rate-limiting, and phosphorylated Whi5 rapidly exits the nucleus. The G1/S regulon, which includes two additional G1 cyclins *CLN1* and *CLN2*, contributes to the activation of B-type cyclins, DNA replication, spindle pole body duplication and bud emergence. Mitotic B-type cyclins then inactivate SBF[20] and, with *NRM1*, inactivate MBF[21], thus turning off the G1/S regulon.

Any one of the three G1 cyclins suffices to activate the regulon, suggesting that there is potential for transcriptional positive feedback of *CLN1* and *CLN2* on their own expression[22,23]. However, analysis of synchronized populations led to the conclusion that positive feedback, defined as Cln1 and Cln2 advancing transcription from the *CLN2* promoter, did not occur in wild type; instead, Cln3 was the sole activator of firing[14,15].

In sharp contrast to the prevailing linear model, we demonstrate that Cln1- and Cln2-dependent positive feedback is central to Start control. We use single-cell time-lapse fluorescent microscopy to show that Cln1 and Cln2 advance timing and reduce variability in the activation of *CLN2*, and of the entire G1/S regulon. We further explore the mechanisms and functional significance of this control.

Positive feedback of G1 cyclins

Positive feedback of Cln1 and Cln2 on their own transcription should yield faster accumulation of *CLN2* messenger RNA in wild-type cells than in *cln1*Δ *cln2*Δ cells. Although Cln1- and Cln2-dependent positive feedback was clearly demonstrated in the absence of Cln3 (refs 22–24), this does not indicate that wild-type cells function similarly. In synchronized populations, near-identical timing of onset of *CLN2* promoter activity was observed in the presence or absence of *CLN1* and *CLN2*, leading to the linear model[14,15]. Here we revisit this issue using single-cell assays. We used unstable green fluorescent protein (GFP) driven by the *CLN2* promoter (*CLN2pr-GFP*) as a reporter for *CLN2* transcription[24,25] (see Methods and Supplementary Figs 1 and 2). Birth time was determined using the disappearance of the Myo1–GFP myosin ring[11], a marker for cytokinesis that did not influence the *CLN2pr-GFP* signal. The timing of *CLN2* promoter induction in individual cells is sharp and easily quantified computationally (see Methods, Fig. 1b–e and Supplementary Figs 1 and 2). Because *cln1*Δ *cln2*Δ cells are larger than wild type, we integrated *MET3pr-CLN2* in both strains to conditionally express Cln2 before time-lapse imaging so that initial sizes were comparable[14] (see Methods and Supplementary Figs 3 and 12 for controls). Thus, we can assay for positive feedback by comparing the time interval from birth to transcriptional activation of *CLN2pr-GFP* transcription in the first cell cycle after *MET3pr-CLN2* is turned off in wild-type and *cln1*Δ *cln2*Δ cells.

Positive feedback should advance *CLN2* promoter activation in wild-type compared to *cln1*Δ *cln2*Δ cells[14,15]. In daughter cells, the average time between birth and *CLN2* promoter activation (τ_{on}; Fig. 1d–f) was much shorter for wild type (41 min) than for *cln1*Δ *cln2*Δ (83 min). Furthermore, *CLN2pr-GFP* activation was much less variable for wild-type than for *cln1*Δ *cln2*Δ cells (standard deviation of 21 min versus 47 min). *CLN2pr-GFP* transcription was Cln3-dependent in *cln1*Δ *cln2*Δ cells because *cln1*Δ *cln2*Δ *cln3*Δ cells failed to induce *CLN2pr-GFP*. Qualitatively similar results were

[1]Center for Studies in Physics and Biology, The Rockefeller University, [2]The Rockefeller University, 1230 York Avenue, New York 10065, USA.

obtained in mother cells and also in cells growing in glycerol and ethanol instead of glucose. In all cases, the interval from birth to *CLN2pr-GFP* activation was smaller and less variable in wild type than in *cln1*Δ *cln2*Δ, indicating strong positive feedback of Cln1 and Cln2 on their own transcription independent of nutrient conditions or cell type (Supplementary Table 3; $P < 10^{-4}$).

We explored the potential redundancy of *CLN1* and *CLN2* in activating the feedback loop. Although budding is slightly delayed in *cln1*Δ *CLN2* and *CLN1 cln2*Δ cells compared to wild type, the timing of *CLN2* promoter activation is similar (Supplementary Table 3), indicating that *CLN1* and *CLN2* form redundant conduits for positive feedback.

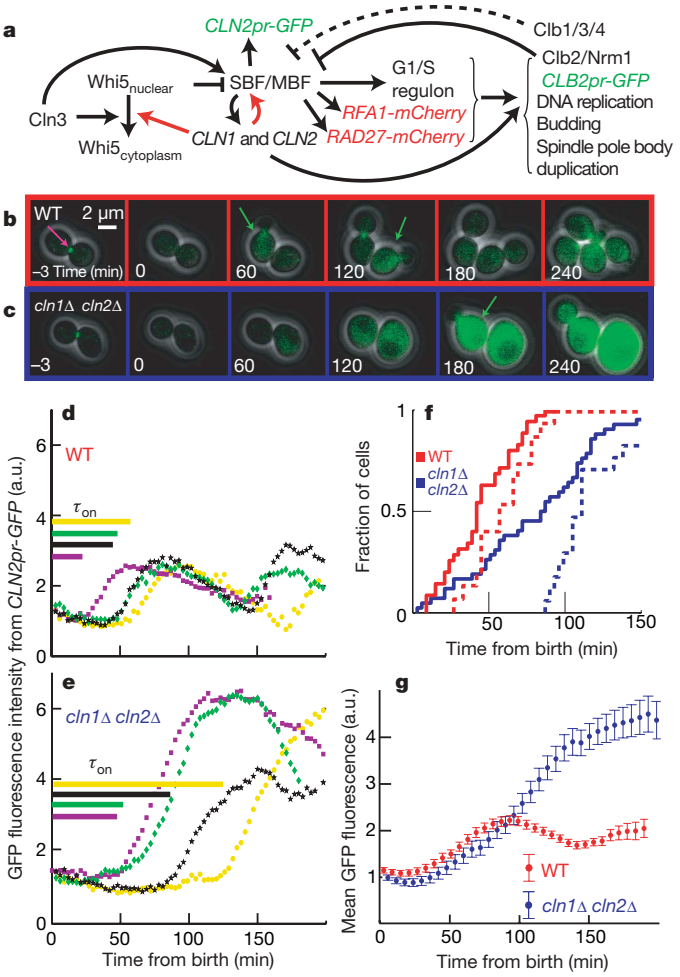

Figure 1 | Positive feedback drives the Start of the budding yeast cell cycle. **a**, Schematic of the Start transition; new interactions demonstrated in this paper are shown in red. **b**, **c**, Combined phase and fluorescence images for *CLN2pr-GFP MYO1-GFP MET3pr-CLN2* cells, either wild type (WT; **b**) or *cln1*Δ *cln2*Δ (**c**), grown without methionine (inducing) and plated on methionine (repressing) to normalize initial conditions[6] (Supplementary Fig. 3). Green arrows indicate approximate peak GFP expression from *CLN2pr-GFP*. **d**, **e**, Single-cell fluorescence intensity (in arbitrary units, a.u.) for four characteristic cells of each genotype; cells are synchronized at birth and marked by the disappearance of a Myo1–GFP ring at the bud-neck (purple arrow in **b**). The time from birth to *CLN2* promoter activation (as defined in Methods), τ_{on}, for each individual cell is indicated by length of the corresponding line. **f**, Cumulative distribution of *CLN2pr-GFP* (solid lines) induction indicates that Cln1- and Cln2-dependent positive feedback contributes substantially to the early expression of *CLN2*; dashed lines indicate induction of *CLB2pr-GFP* marking the onset of negative regulation of *CLN2*. **g**, Average fluorescence intensity for 87 wild-type and 83 *cln1*Δ *cln2*Δ daughter cells aligned at birth simulates a population study, which would obscure the effect of positive feedback. The results shown are for daughter cells in glucose; changes in cell type or nutrient conditions do not qualitatively influence the results (Supplementary Table 3). Error bars, s.e.m.

Our data can be reconciled with previous work[14,15] arguing against positive feedback because measurements averaged over a population of cells necessarily lose information. In addition to delayed onset of transcription, *cln1*Δ *cln2*Δ cells express a more intense and prolonged *CLN2pr-GFP* signal. The larger peaks are probably due to a delay in the Clb2-mediated repression of SBF/MBF[14,15,20,21] (Fig. 1d, e), because the average time between induction of *CLN2* and *CLB2* was much larger in *cln1*Δ *cln2*Δ strains (measured using a *CLB2pr-GFP* cassette; Fig. 1f and Supplementary Fig. 13), and Clb2 accumulation is known to be delayed in *cln1*Δ *cln2*Δ strains[14].

Therefore, imperfect synchrony[11] allows the high and lengthened transcriptional response from the first *cln1*Δ *cln2*Δ cells firing the *CLN2* promoter to mask the delayed response of the majority. This effect is reconstituted in Fig. 1g by averaging our measured single-cell data, and explains why positive feedback was not detected in measurements of mRNA levels in populations of synchronized daughter cells[14,15].

Coherent regulon expression

Once a cell senses the signal to initiate the cell cycle, it must actuate all the machinery effecting the cell cycle transition. At Start, this requires activation of many SBF- and MBF-regulated genes[16] encoding proteins involved in DNA replication and bud-site formation. However, noise in protein expression in individual cells[26] could interfere with expression of this large regulon. In particular, the delayed and variable induction of the *CLN2* promoter in *cln1*Δ *cln2*Δ cells suggested that G1/S regulon expression might be severely disrupted in these feedback-free cells.

To investigate regulon expression in individual cells, we compared induction of *CLN2pr-GFP* and *RAD27-mCherry*, another member of the regulon[16] (Fig. 2a–d and Supplementary Figs 7 and 8). *RAD27* expression is Cln-dependent (Supplementary Fig. 11). *CLN2* and *RAD27* are synchronously induced in wild type, whereas there is a long and variable period of time between the inductions of the two genes in the *cln1*Δ *cln2*Δ mutant (Fig. 2e, f). Out of the 86 *cln1*Δ *cln2*Δ cells studied, 11 failed to produce a detectable increase in Rad27–mCherry and 4 failed to produce a detectable increase of either marker. We performed identical experiments on strains containing *CLN2pr-GFP* and *RFA1-mCherry*, another regulon member[16], and obtained similar results (Fig. 2g, h). Our conclusions are valid even after excluding outlying points ($P < 0.01$). Thus, Cln1- and Cln2-dependent positive feedback probably promotes coherent and efficient transcription across the SBF/MBF regulon.

Further comparison of these three promoters in *cln1*Δ *cln2*Δ cells reveals that *CLN2* is almost always the first of the three to be activated, whereas the times to subsequent *RFA1pr* and *RAD27pr* inductions are significantly different from each other ($P = 0.004$; Supplementary Table 3). This suggests that the *CLN2* promoter is the easiest for Cln3 to induce, followed by the *RFA1* promoter and then the *RAD27* promoter. We note that two MBF targets[27–29], *RAD27* and *RFA1*, show different induction timing.

To address whether the lack of coherence in *cln1*Δ *cln2*Δ cells simply comes from low G1 cyclin levels, we analysed *cln1*Δ *cln2*Δ 6×*CLN3* cells (containing an extra five tandem integrated copies of *CLN3*). Although the expression of both the *CLN2* and *RAD27* promoters was significantly accelerated by extra *CLN3*, these cells still showed strongly incoherent expression compared to wild type (Fig. 2i).

To directly short-circuit the proposed positive feedback loop, we examined gene expression in *cln1*Δ *cln2*Δ *cln3*Δ *MET3pr-CLN2* cells on methionine-free medium (*MET3pr-CLN2* on). Although induction of *CLN2pr-GFP* and *RAD27-mCherry* was strongly accelerated by constitutive *CLN2* expression, incoherent expression compared to wild type was still observed (Fig. 2j). Notably, this incoherence was due to *RAD27-mCherry* induction before *CLN2pr-GFP*, compared to nearly simultaneous expression in wild type (−8 ± 2 min compared

to 2 ± 1 min (mean ± s.e.m.); $P < 10^{-3}$), perhaps owing to differential loading of SBF (*CLN2*) and MBF (*RAD27*) regulated genes[21,27–30].

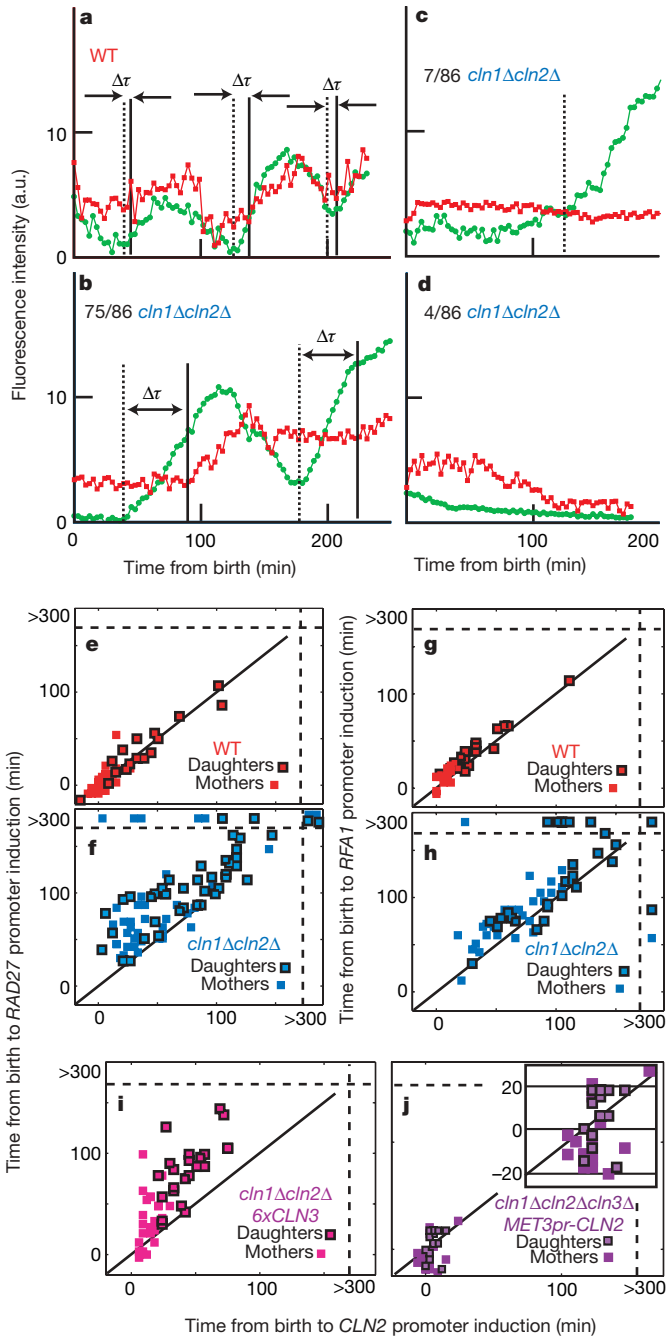

Figure 2 | Cln1 and Cln2 drive coherent expression of the SBF/MBF regulon. a–f, Strains containing both *CLN2pr-GFP* (green) and *RAD27-mCherry* (red) were examined (see Supplementary Information); τ marks the computed time between *CLN2* and *RAD27* inductions. In wild type (**a**, **e**), all cells transcribed both markers synchronously; in *cln1Δ cln2Δ* (**b–d**, **f**), 75 cells transcribed both markers, with variable intervening intervals; 7 cells transcribed *CLN2pr-GFP* but not *RAD27-mCherry*; and 4 cells transcribed neither. Correlation of the initiation of *RAD27* and *CLN2* transcription in wild type (**e**) and *cln1Δ cln2Δ* (**f**) is shown; points beyond the dotted lines in (**f**, **h**) represent no transcription within 300 min (movie limit; see also Supplementary Table 3). **g**, **h**, Substituting *RFA1-mCherry* for *RAD27-mCherry* yielded similar results. **i**, **j**, *cln1Δ cln2Δ* 6xCLN3 cells (**i**) and *cln1Δ cln2Δ cln3Δ* cells expressing *CLN2* from a *MET3* promoter (**j**) exhibited incoherent regulon expression compared to wild type, although expression of both *CLN2pr* and *RAD27pr* were faster than in *cln1Δ cln2Δ*. $P < 10^{-3}$ for all comparisons.

Overall, these experiments suggest that the positive feedback architecture is a particularly effective way to promote coherent regulon expression.

Stochastic cell cycle arrest

In addition to showing incoherent gene expression, 26% of *cln1Δ cln2Δ* cells fail to bud (Fig. 3a). We hypothesized that incoherent gene expression has a role in this sporadic unbudded arrest. Twenty out of 143 assayed *cln1Δ cln2Δ* cells were 'strongly incoherent': they failed to transcribe one or both of their two transcriptional markers (Fig. 2f, h); 90% of the strongly incoherent cells arrested unbudded, compared to 26% of all *cln1Δ cln2Δ* cells ($P < 0.003$; Fig. 3a). Thus, a lack of coherence in the SBF/MBF regulon is a strong predictor of unbudded arrest within the *cln1Δ cln2Δ* population. *6xCLN3* reduced unbudded arrest in *cln1Δ cln2Δ* cells, perhaps because of accelerated regulon expression (Fig. 2i). Thus, unbudded arrest in *cln1Δ cln2Δ* cells may result from highly delayed expression of some regulon members.

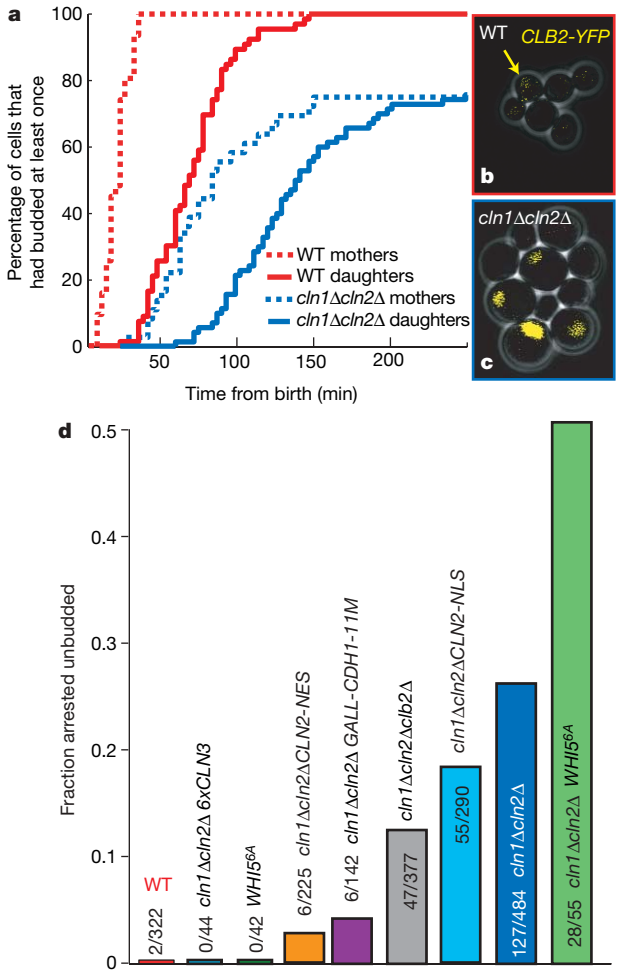

Figure 3 | Stochastic unbudded arrest in *cln1Δ cln2Δ* cells and its modulation by Cln2, Cln3, Whi5, and the mitotic cyclins. a, A cumulative plot of the percentage of cells that budded at least once; 26% of *cln1Δ cln2Δ* cells arrest unbudded. **b**, **c**, Wild-type (**b**) and *cln1Δ cln2Δ* (**c**) cells with integrated *CLB2-YFP* fusion protein (endogenous promoter). Note that there is high nuclear Clb2 specifically in large unbudded (arrested) *cln1Δ cln2Δ* cells. **d**, Delaying (*cln1Δ cln2Δ clb2Δ*) or removing (*cln1Δ cln2Δ GALL-CDH1-11M*) mitotic cyclin accumulation reduced the fraction of arrested cells; the addition of five copies of *CLN3* (*6xCLN3*) eliminated this arrest, whereas the addition of $WHI5^{6A}$ exacerbated the arrest. Unbudded arrest was weakly rescued by nuclear Cln2 (*CLN2-NLS*), and strongly rescued by cytoplasmic Cln2 (*CLN2-NES*). Unless stated otherwise in the text, $P < 10^{-3}$ for all comparisons.

We hypothesized that in strongly incoherent cells, activation of only some regulon members might lead to activation of mitotic Clbs, which would then inactivate further SBF/MBF-regulated expression[20] (Fig. 1a and Supplementary Fig. 9). If the genes required for budding in the absence of *CLN1* and *CLN2*, such as *PCL1* and *PCL2* (ref. 31), had not yet been expressed by the time of Clb activation, unbudded arrest might ensue. Indeed, 20 out of 20 arrested *cln1*Δ *cln2*Δ cells contained large amounts of nuclear Clb2–yellow fluorescent protein (YFP) (Fig. 3b, c).

To test the role of transcription in unbudded arrest further, we deleted the rate-limiting SBF inhibitor *CLB2* in a *MET3pr-CLN2 cln1*Δ *cln2*Δ strain and observed a decrease in unbudded arrest from 26% to 13% (Fig. 3d). Additionally, we integrated unphosphorylatable Cdh1 under galactose control (*GALL-HA3-CDH1-m11*) into a *cln1*Δ *cln2*Δ *MET3pr-CLN2* strain to induce rapid degradation of all mitotic cyclins on galactose induction[32]. This reduced the unbudded arrested fraction to 4% in the first cell cycle after galactose induction (Fig. 3d). Because the timing of *CLB2pr-GFP* induction in *cln1*Δ *cln2*Δ cells was similar whether they arrested or not ($P = 0.91$), the unbudded arrest was not due to unusually early *CLB2* induction.

Thus, mitotic cyclins promote unbudded arrest specifically in highly incoherent *cln1*Δ *cln2*Δ cells, probably owing to insufficient regulon expression before Clb-dependent SBF/MBF inactivation.

Cln1 and Cln2 inactivate the transcriptional inhibitor *WHI5*

We wanted to determine if Cln1- and Cln2-dependent positive feedback operated through Whi5, a transcriptional inhibitor of the G1/S regulon[18,19]. Whi5 inactivation is rate-limiting for *CLN2* transcription and occurs by means of Cln-dependent phosphorylation, which leads to nuclear exclusion[19].

First, we developed a quantitative assay for nuclear levels of Whi5–GFP by marking the nucleus with *HTB2-mCherry* (histone H2B) and measuring the difference between nuclear and cytoplasmic GFP fluorescence intensity (Fig. 4a–c). Whi5 entered the nucleus rapidly in both wild-type and *cln1*Δ *cln2*Δ cells. In wild-type cells, Whi5 also exited very rapidly; in *cln1*Δ *cln2*Δ cells, Whi5 exited much more slowly (Fig. 4d–g, i) consistent with biochemical data showing that Whi5 remains on the *CLN2* promoter longer in *cln1*Δ *cln2*Δ than in wild-type cells[18]. Because Whi5–GFP remained nuclear in *cln1*Δ *cln2*Δ *cln3*Δ cells (Fig. 4h), the slow Whi5 exit in *cln1*Δ *cln2*Δ cells is Cln3-dependent (this also excludes photobleaching artefacts). Thus, Cln3 initiates the slow exit of Whi5 from the nucleus, whereas Cln1 and Cln2 rapidly remove the remainder.

Because Whi5 exit and *CLN2* induction are tightly correlated in wild-type cells (Fig. 4j), translocation occurs shortly after Whi5 inactivation and coincides with activation of transcriptional positive feedback. *CLN2* promoter activation and Whi5 exit were less tightly correlated in *cln1*Δ *cln2*Δ cells consistent with the gradual exit of Whi5 (Fig. 4k and Supplementary Figs 5 and 6).

To examine the role of Whi5 phosphorylation in positive feedback and regulon coherence, we used a *WHI5*^{6A} allele[19] lacking 6 of the 12 Cln-dependent phosphorylation sites. Although Whi5^{6A} was reported to be constitutively nuclear[19], we observed significant, but slower and incomplete, shuttling of Whi5^{6A}–GFP out of the nucleus at Start and again at nuclear division (10 out of 10 cells; Fig. 4l). *CLN2* and *RAD27* induction are less coherent in *WHI5*^{6A} than in wild type (Fig. 4m; but

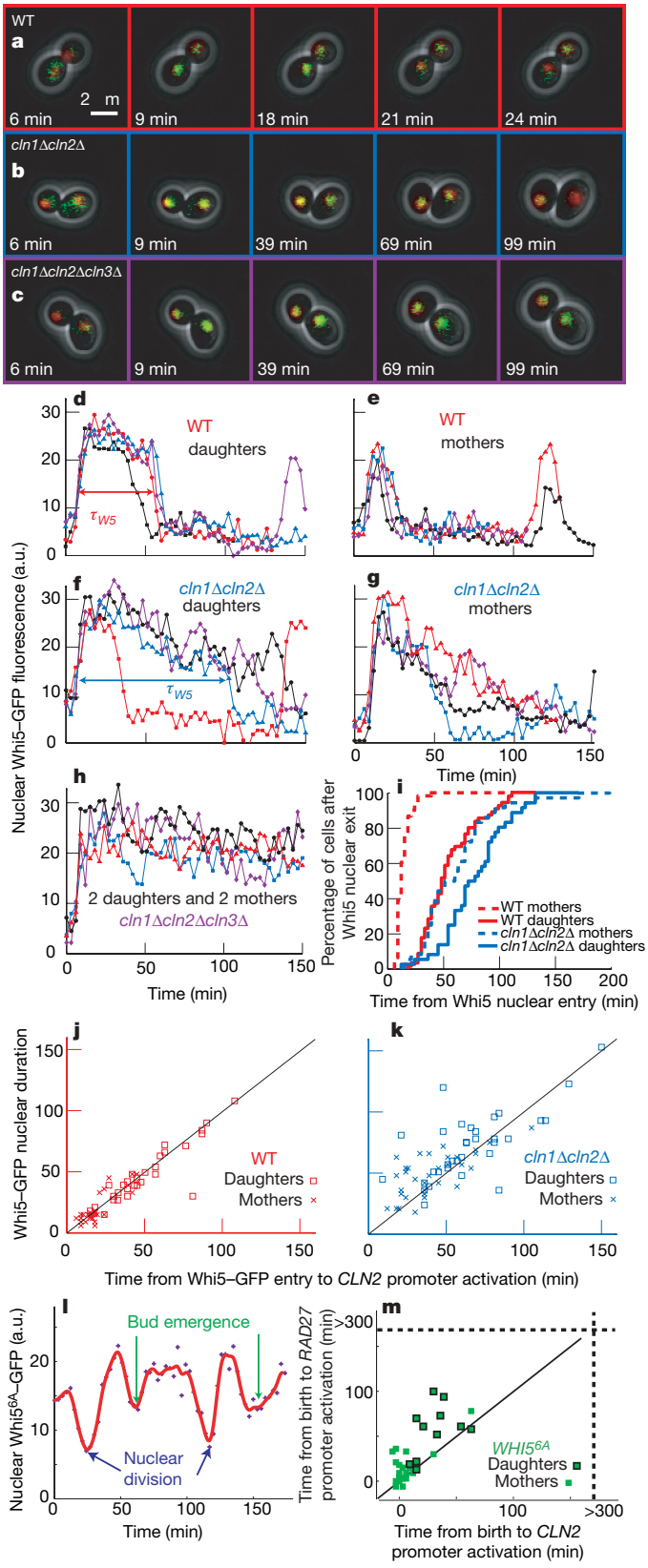

Figure 4 | Cln1 and Cln2 are required for rapid phosphorylation and inactivation of the rate-limiting inhibitor Whi5. **a–c**, Combined phase and fluorescence images showing Whi5–GFP and Htb2–mCherry (to mark the nucleus) fusion proteins for wild-type (**a**), *cln1*Δ *cln2*Δ (**b**) and *cln1*Δ *cln2*Δ *cln3*Δ (**c**) cells. The difference between nuclear and non-nuclear fluorescence intensity was used to quantify nuclear Whi5 by automated image analysis. **d–h**, Nuclear Whi5–GFP fluorescence. In comparison to wild-type cells (**d**, **e**), *cln1*Δ *cln2*Δ cells display delayed and less sharp Whi5 nuclear exit (**f**, **g**). Whi5 remains nuclear in *cln1*Δ *cln2*Δ *cln3*Δ cells (**h**). **i**, The percentage of cells in which Whi5 has left the nucleus (defined as attaining half the maximum amount) versus the time from Whi5 nuclear entry. **j**, **k**, Whi5 nuclear exit is tightly correlated with *CLN2* promoter activation in wild-type cells and less correlated in *cln1*Δ *cln2*Δ cells (see also Supplementary Table 3). **l**, Whi5^{6A}–GFP (ref. 19), lacking 6 out of 12 Cln-dependent phosphorylation sites, reproducibly displayed significant, but slower and incomplete, shuttling out of the nucleus at Start and again at nuclear division. **m**, In *WHI5*^{6A} strains containing *CLN2pr-GFP* and *RAD27-mCherry*, *CLN2* and *RAD27* induction were incoherent, correlating with the poor nuclear transport of Whi5^{6A}–GFP.

more coherent than *cln1Δ cln2Δ*), correlating with the poor nuclear transport of Whi5[6A]. Thus, interfering with the positive feedback loop by reducing the ability of Cln proteins to phosphorylate Whi5 reduces regulon coherence, even with all three G1 cyclins present.

The addition of *WHI5*[6A] to *cln1Δ cln2Δ* cells increased the frequency of unbudded arrest from 26% to 51%, consistent with the idea that unbudded arrest is a consequence of incoherent regulon expression in *cln1Δ cln2Δ* cells.

Overall, these results indicate that Whi5 is a Cln1 and Cln2 substrate in wild-type cells, and that this phosphorylation contributes to positive feedback. To determine whether Whi5 was the only such substrate, we compared timing of *CLN2* promoter activation for *whi5Δ* and *cln1Δ cln2Δ whi5Δ* cells (Supplementary Fig. 14 and Supplementary Table 3). Deletion of *WHI5* advances *CLN2* promoter induction in both wild-type and *cln1Δ cln2Δ* cells. Because *cln1Δ cln2Δ whi5Δ* cells delayed *CLN2pr* induction relative to *CLN1 CLN2 whi5Δ* cells, Cln1 and Cln2 probably act through Whi5-dependent and -independent mechanisms to promote positive feedback. Previous results indicated a Whi5-independent Cln3 requirement for SBF activation[19], possibly acting through Swi6 (refs 19 and 33); a similar mechanism may be used by Cln1 and Cln2.

Separable Cln2 functions

Cln1 and Cln2 are pleiotropic effectors of Start that have important nuclear and cytoplasmic functions[34,35], complicating the interpretation of *cln1Δ cln2Δ* phenotypes. Therefore, we tested forced-localization *CLN2* alleles, expressed from the wild-type *CLN2* promoter, that restrict Cln2 to either the nucleus (*CLN2-NLS*) or the cytoplasm (*CLN2-NES*)[34]. *cln1Δ cln2Δ CLN2-NLS* cells show coherent regulon expression ($P = 0.45$ compared to wild type), but *cln1Δ cln2Δ CLN2-NES* cells are highly incoherent compared to wild type ($P < 10^{-7}$); this indicates that coherent gene expression is primarily a nuclear function of *CLN2* (Fig. 5a, b (compare to Fig. 2), and Supplementary Table 3).

Consistent with a role of cytoplasmic Cln2 in budding[34,35], integration of *CLN2-NES* into *cln1Δ cln2Δ* cells strongly reduces arrest (to 3%) in spite of less coherent gene expression. Furthermore, exogenous expression of *CLN2* drives cell cycle progression in previously blocked *cln1Δ cln2Δ* cells (Supplementary Fig. 10) and restores viability of *mbp1Δ swi4Δ* cells, which lack SBF and MBF and have very low regulon expression[36,37]. The localization mutants also have different efficacy for relieving unbudded arrest. Integration of *CLN2-NLS* into *cln1Δ cln2Δ* cells, providing coherent gene expression, led to a partial but significant reduction of unbudded arrest (from 26% to 19%; $P = 0.04$).

Thus, cell morphogenesis and budding can be driven by two partially redundant pathways: by cytoplasmic Cln1 and Cln2 (refs 34 and 38), or by other genes in the G1/S regulon such as *PCL1* and *PCL2* (ref. 31; Fig. 5c). Having Cln1 and Cln2 coherently activate the G1/S regulon and directly drive bud emergence provides a compact solution to ensure efficient and timely morphogenesis and G1/S regulon expression, before subsequent Clb activation.

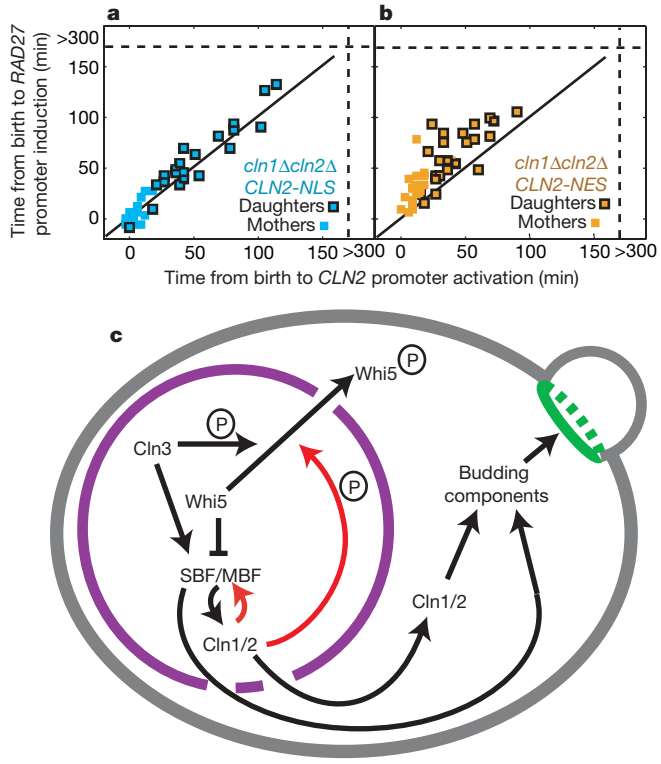

Figure 5 | Function of nuclear Cln2 and a model for Start regulation by positive feedback. **a**, **b**, Comparison of *cln1Δ cln2Δ* cells with either a nuclear localized (**a**) or a nuclear excluded (**b**) *CLN2* allele suggests that nuclear Cln2 is necessary and sufficient for regulon coherence. Strains contained *CLN2pr-GFP* and *RAD27-mCherry*. **c**, Model for regulon activation and bud emergence; red lines indicate pathways generating positive feedback.

Discussion

The regulatory architecture of the G1/S regulon provides an effective design to promote coordinated activation. The promoters are preloaded during G1 with a complex of factors that are subsequently rapidly activated by phosphorylation[17,24,30], removing a potentially rate-limiting step. Furthermore, the upstream cyclin Cln3 is intrinsically more capable of triggering the *CLN2* promoter compared to two other randomly selected promoters from the regulon (*RFA1* or *RAD27*; Fig. 2e–h). The high sensitivity of *CLN1* and *CLN2* to Cln3 means that positive feedback from the initial burst of Cln1 and Cln2 will ensure that all other genes fire together. Indeed, in our experiments in wild-type cells, the genes are expressed too synchronously to evaluate which comes first. We find it probable that positive feedback will be a recurring motif in genetic control networks responsible for the coherent temporal coordination of multiple downstream events.

The sharpness of the Start switch, defined by the rapid exclusion of the transcriptional inhibitor Whi5 and the coherent expression of the G1/S regulon, is principally due to *CLN1*- and *CLN2*-dependent positive feedback (Fig. 5c, red lines) rather than a linear Cln3–Whi5–SBF pathway[14,15,18,19]. Our data are inconsistent with the sharpness of Start being primarily due to nonlinear increases in *CLN3* translation[39] or nuclear translocation[40], or cooperative phosphorylation of Whi5 by Cln3 (ref. 19), because these mechanisms all predict a sharp switch in feedback-free *cln1Δ cln2Δ* cells.

In budding yeast, Start is a fundamental point of commitment at which physiological inputs such as nutrients, mating factor, size and cell type are integrated to produce an all-or-none decision. We show here that positive feedback provides robust switch-like cell cycle entry. Our single-cell data suggest that the point of commitment to the cell cycle, Start, is a very brief interval coinciding with the initiation of positive feedback and Whi5 exclusion. Subsequent Cln-dependent events, such as Sic1 phosphorylation and degradation[41] leading to DNA replication, could then be viewed as dependent on, rather than part of, Start.

This work also provides a molecular basis for understanding the modular structure of G1 (ref. 11). Two temporally uncorrelated processes in G1 are separated by the molecular event of Whi5 inactivation and nuclear exit. The upstream module is responsible for cell size control, whereas the downstream size-independent module actuates cell cycle progression[11]. Here, we showed that rapid Whi5 exit coincided with initiation of Cln1- and Cln2-dependent positive feedback. Once feedback is initiated, the rapidly accumulating Cln1 and Cln2 probably dominate cellular Cln-kinase activity, and Cln3, the rate-limiting upstream activator, is rendered unimportant. In general, we expect modularity, best shown by single-cell analysis, to be a signature of feedback-driven cellular control networks.

Our systems-level analysis of Start provides a template for further studies of other checkpoints in yeasts or the G1/S transition in mammals. The utility of feedback at Start leads us to expect similar regulatory architecture across eukaryotes, even if the enabling genes are not homologous.

METHODS SUMMARY

Strain and plasmid constructions. Standard methods were used throughout. All strains are W303-congenic.

Time-lapse microscopy. Preparation of cells for time-lapse microscopy was performed as previously described[24]. We integrated *MET3pr-CLN2* to conditionally express Cln2 (ref. 14). By pre-growing cells without methionine before plating on media containing methionine (*MET3pr-CLN2* off), we were able to begin our time-lapse imaging experiments with similarly sized wild-type and *cln1*Δ *cln2*Δ cells. We imaged the first Start in cells that were budded at the time of transfer and that divided at least 30 min after methionine addition, to allow degradation of Cln2 (refs 13 and 42) synthesized before *MET3* promoter turn-off.

Image analysis. Automated image segmentation and fluorescence quantification of yeast grown under time-lapse conditions were performed as previously described[11,24]. We added a function to previously described custom software[24] to identify nuclei labelled with Htb2–mCherry (histone H2B).

Data analysis. Fluorescence time series were extracted from movies as previously described[24]. Time series were fit using smoothing splines (Matlab) with a smoothing parameter of 0.001. We defined the onset of transcription for a G1/S fluorescent reporter by the maximum in the second derivative that fell between birth and budding (scored separately), which accurately locates rate changes in spite of noisy data and slow changes in the background fluorescence (Supplementary Figs 3 and 4).

Full Methods and any associated references are available in the online version of the paper at www.nature.com/nature.

Received 15 January; accepted 29 May 2008.

1. Simchen, G., Pinon, R. & Salts, Y. Sporulation in *Saccharomyces cerevisiae*: premeiotic DNA synthesis, readiness and commitment. *Exp. Cell Res.* **75,** 207–218 (1972).
2. Nachman, I., Regev, A. & Ramanathan, S. Dissecting timing variability in yeast meiosis. *Cell* **131,** 544–556 (2007).
3. Shenhar, G. & Kassir, Y. A positive regulator of mitosis, Sok2, functions as a negative regulator of meiosis in *Saccharomyces cerevisiae*. *Mol. Cell. Biol.* **21,** 1603–1612 (2001).
4. Ferrell, J. E. Jr & Machleder, E. M. The biochemical basis of an all-or-none cell fate switch in *Xenopus* oocytes. *Science* **280,** 895–898 (1998).
5. Xiong, W. & Ferrell, J. E. Jr. A positive-feedback-based bistable 'memory module' that governs a cell fate decision. *Nature* **426,** 460–465 (2003).
6. Sha, W. *et al.* Hysteresis drives cell-cycle transitions in *Xenopus laevis* egg extracts. *Proc. Natl Acad. Sci. USA* **100,** 975–980 (2003).
7. Pomerening, J. R., Sontag, E. D. & Ferrell, J. E. Jr. Building a cell cycle oscillator: hysteresis and bistability in the activation of Cdc2. *Nature Cell Biol.* **5,** 346–351 (2003).
8. Hartwell, L. H., Culotti, J., Pringle, J. R. & Reid, B. J. Genetic control of the cell division cycle in yeast. *Science* **183,** 46–51 (1974).
9. Johnston, G. C., Pringle, J. R. & Hartwell, L. H. Coordination of growth with cell division in the yeast *Saccharomyces cerevisiae*. *Exp. Cell Res.* **105,** 79–98 (1977).
10. Lord, P. G. & Wheals, A. E. Variability in individual cell cycles of *Saccharomyces cerevisiae*. *J. Cell Sci.* **50,** 361–376 (1981).
11. Di Talia, S., Skotheim, J. M., Bean, J. M., Siggia, E. D. & Cross, F. R. The effects of molecular noise and size control on variability in the budding yeast cell cycle. *Nature* **448,** 947–951 (2007).
12. Jorgensen, P. & Tyers, M. How cells coordinate growth and division. *Curr. Biol.* **14,** R1014–R1027 (2004).
13. Tyers, M., Tokiwa, G. & Futcher, B. Comparison of the *Saccharomyces cerevisiae* G_1 cyclins: Cln3 may be an upstream activator of Cln1, Cln2 and other cyclins. *EMBO J.* **12,** 1955–1968 (1993).
14. Dirick, L., Bohm, T. & Nasmyth, K. Roles and regulation of Cln–Cdc28 kinases at the start of the cell cycle of *Saccharomyces cerevisiae*. *EMBO J.* **14,** 4803–4813 (1995).
15. Stuart, D. & Wittenberg, C. CLN3, not positive feedback, determines the timing of CLN2 transcription in cycling cells. *Genes Dev.* **9,** 2780–2794 (1995).
16. Spellman, P. T. *et al.* Comprehensive identification of cell cycle-regulated genes of the yeast *Saccharomyces cerevisiae* by microarray hybridization. *Mol. Biol. Cell* **9,** 3273–3297 (1998).
17. Kato, M., Hata, N., Banerjee, N., Futcher, B. & Zhang, M. Q. Identifying combinatorial regulation of transcription factors and binding motifs. *Genome Biol.* **5,** R56 (2004).
18. de Bruin, R. A., McDonald, W. H., Kalashnikova, T. I., Yates, J. III & Wittenberg, C. Cln3 activates G1-specific transcription via phosphorylation of the SBF bound repressor Whi5. *Cell* **117,** 887–898 (2004).
19. Costanzo, M. *et al.* CDK activity antagonizes Whi5, an inhibitor of G1/S transcription in yeast. *Cell* **117,** 899–913 (2004).
20. Amon, A., Tyers, M., Futcher, B. & Nasmyth, K. Mechanisms that help the yeast cell cycle clock tick: G2 cyclins transcriptionally activate G2 cyclins and repress G1 cyclins. *Cell* **74,** 993–1007 (1993).
21. de Bruin, R. A. *et al.* Constraining G1-specific transcription to late G1 phase: the MBF-associated corepressor Nrm1 acts via negative feedback. *Mol. Cell* **23,** 483–496 (2006).
22. Cross, F. R. & Tinkelenberg, A. H. A potential positive feedback loop controlling CLN1 and CLN2 gene expression at the start of the yeast cell cycle. *Cell* **65,** 875–883 (1991).
23. Dirick, L. & Nasmyth, K. Positive feedback in the activation of G1 cyclins in yeast. *Nature* **351,** 754–757 (1991).
24. Bean, J. M., Siggia, E. D. & Cross, F. R. Coherence and timing of cell cycle Start examined at single-cell resolution. *Mol. Cell* **21,** 3–14 (2006).
25. Mateus, C. & Avery, S. V. Destabilized green fluorescent protein for monitoring dynamic changes in yeast gene expression with flow cytometry. *Yeast* **16,** 1313–1323 (2000).
26. Samoilov, M. S., Price, G. & Arkin, A. P. From fluctuations to phenotypes: the physiology of noise. *Sci. STKE* **2006,** re17 (2006).
27. Iyer, V. R. *et al.* Genomic binding sites of the yeast cell-cycle transcription factors SBF and MBF. *Nature* **409,** 533–538 (2001).
28. Harbison, C. T. *et al.* Transcriptional regulatory code of a eukaryotic genome. *Nature* **431,** 99–104 (2004).
29. Simon, I. *et al.* Serial regulation of transcriptional regulators in the yeast cell cycle. *Cell* **106,** 697–708 (2001).
30. Koch, C., Schleiffer, A., Ammerer, G. & Nasmyth, K. Switching transcription on and off during the yeast cell cycle: Cln/Cdc28 kinases activate bound transcription factor SBF (Swi4/Swi6) at Start, whereas Clb/Cdc28 kinases displace it from the promoter in G_2. *Genes Dev.* **10,** 129–141 (1996).
31. Moffat, J. & Andrews, B. Late-G1 cyclin-CDK activity is essential for control of cell morphogenesis in budding yeast. *Nature Cell Biol.* **6,** 59–66 (2004).
32. Zachariae, W., Schwab, M., Nasmyth, K. & Seufert, W. Control of cyclin ubiquitination by CDK-regulated binding of Hct1 to the anaphase promoting complex. *Science* **282,** 1721–1724 (1998).
33. Wijnen, H., Landman, A. & Futcher, B. The G_1 cyclin Cln3 promotes cell cycle entry via the transcription factor Swi6. *Mol. Cell. Biol.* **22,** 4402–4418 (2002).
34. Edgington, N. P. & Futcher, B. Relationship between the function and the location of G1 cyclins in *S. cerevisiae*. *J. Cell Sci.* **114,** 4599–4611 (2001).
35. Miller, M. E. & Cross, F. R. Distinct subcellular localization patterns contribute to functional specificity of the Cln2 and Cln3 cyclins of *Saccharomyces cerevisiae*. *Mol. Cell. Biol.* **20,** 542–555 (2000).
36. Koch, C., Moll, T., Neuberg, M., Ahorn, H. & Nasmyth, K. A role for the transcription factors Mbp1 and Swi4 in progression from G1 to S phase. *Science* **261,** 1551–1557 (1993).
37. Bean, J. M., Siggia, E. D. & Cross, F. R. High functional overlap between MBF and SBF in the G1/S transcriptional program in *Saccharomyces cerevisiae*. *Genetics* **171,** 49–61 (2005).
38. McCusker, D. *et al.* Cdk1 coordinates cell-surface growth with the cell cycle. *Nature Cell Biol.* **9,** 506–515 (2007).
39. Polymenis, M. & Schmidt, E. V. Coupling of cell division to cell growth by translational control of the G_1 cyclin *CLN3* in yeast. *Genes Dev.* **11,** 2522–2531 (1997).
40. Wang, H., Gari, E., Verges, E., Gallego, C. & Aldea, M. Recruitment of Cdc28 by Whi3 restricts nuclear accumulation of the G1 cyclin–Cdk complex to late G1. *EMBO J.* **23,** 180–190 (2004).
41. Schneider, B. L., Yang, Q. H. & Futcher, A. B. Linkage of replication to Start by the Cdk inhibitor Sic1. *Science* **272,** 560–562 (1996).
42. Lanker, S., Valdivieso, M. H. & Wittenberg, C. Rapid degradation of the G_1 cyclin Cln2 induced by CDK-dependent phosphorylation. *Science* **271,** 1597–1601 (1996).
43. Shaner, N. C. *et al.* Improved monomeric red, orange and yellow fluorescent proteins derived from *Discosoma* sp. red fluorescent protein. *Nature Biotechnol.* **22,** 1567–1572 (2004).

Supplementary Information is linked to the online version of the paper at www.nature.com/nature.

Acknowledgements This work was supported by the National Institute of Health (J.M.S., E.D.S. and F.R.C.), the Burroughs Wellcome Fund (J.M.S.) and the National Science Foundation (E.D.S.). We thank N. Buchler, G. Charvin, B. Drapkin and J. E. Ferrell for conversations; J. Widom and C. Wittenberg for comments on the manuscript; J. M. Bean, B. Timney and J. Robbins for help with strain/plasmid construction; M. Schwab for the plasmid pWS358; B. Futcher for the *CLN2-NES* and *CLN2-NLS* plasmids; E. Bi for the pKT355 mCherry tagging plasmid; and M. Tyers for *WHI5* phosphorylation site mutant strains and plasmids.

Author Information Reprints and permissions information is available at www.nature.com/reprints. Correspondence and requests for materials should be addressed to J.M.S. (skotheim@stanford.edu).

METHODS

Strain and plasmid constructions. Standard methods were used throughout. All strains are W303-congenic. In synchronized wild-type cells, *GFP* mRNA from the *CLN2* promoter and *CLN2* mRNA follow similar kinetics, and accumulation of cellular fluorescence follows with a slight delay[24]. *WHI5*^{6A} and *WHI5*^{6A}*-GFP* strains with modified *WHI5* at the endogenous locus were a gift from M. Tyers. Plasmids for introduction of *CLN2-NES* and *CLN2-NLS* under control of the *CLN2* promoter were obtained from B. Futcher, and integrated at the *ura3* locus in a *cln1*Δ *cln2*Δ background. Histone H2B (*HTB2*) was carboxy-terminally tagged with *mCherry* using PCR-mediated tagging with the template plasmid pKT355 (ref. 43). *RAD27* and *RFA1* were tagged similarly. All other alleles were from laboratory stocks described previously.

Time-lapse microscopy. Preparation of cells for time-lapse microscopy was performed as previously described[24]. Because mutant cells are larger than wild type, we integrated *MET3pr-CLN2* to conditionally express Cln2 (ref. 14). On media lacking methionine (*MET3pr-CLN2* on), cells bud and divide at comparable sizes (Supplementary Fig. 3). By pre-growing cells without methionine before plating on media containing methionine (*MET3pr-CLN2* off), we were able to begin our time-lapse imaging experiments with similarly sized wild-type and *cln1*Δ *cln2*Δ cells. We imaged the first Start in cells that were budded at the time of transfer and that divided at least 30 min after methionine addition, to allow degradation of Cln2 (refs 13 and 42) that was synthesized before *MET3* promoter turn-off. In brief, growth of microcolonies was observed with fluorescence time-lapse microscopy at 30 °C using a Leica DMIRE2 inverted microscope with a Ludl motorized XY stage. Images were acquired every 3 min for cells grown in glucose and every 6 min for cells grown in glycerol/ethanol with a Hamamatsu Orca-ER camera. Custom Visual Basic software integrated with ImagePro Plus was used to automate image acquisition and microscope control.

Image analysis. Automated image segmentation and fluorescence quantification of yeast grown under time-lapse conditions were performed as previously described[24]. Budding was scored visually, and cell birth was scored by the disappearance of Myo1–GFP at the bud neck, generally with single-frame accuracy. Background was measured as the average fluorescence of unlabelled cells and subtracted from the measured pixel intensities. We added a function to previously described custom software[24] to identify nuclei labelled with Htb2–mCherry (histone H2B). The red signal was smoothed, disconnected fragments were eliminated and the cells with nuclei that were too small, dim or oddly shaped (area versus minimally enclosed rectangle) were eliminated. After background subtraction, the nucleus was defined to be where the fluorescence was greater than 70% of maximum, which controls for cell variability and vertical movement of the nucleus. The nuclear Whi5–GFP signal was the difference between the average nuclear and cytosolic intensities.

Data analysis. *P* values using appropriate tests yielded $P < 0.001$ for all comparisons in the text, except where noted. Fluorescence time series were extracted from movies as previously described[24]. Time series were fit using smoothing splines (Matlab) with a smoothing parameter of 0.001. We defined the onset of transcription for a G1/S fluorescent reporter by the maximum in the second derivative that fell between birth and budding (scored separately). This method was chosen because it accurately locates rate changes in spite of noisy data and slow changes in the background fluorescence. The onset time was nearly unchanged over a range of 10^3 in smoothing parameter (Supplementary Figs 3 and 4).